Journal of Natural Fibers

ISSN: 1544-0478 (Print) 1544-046X (Online) Journal homepage: www.tandfonline.com/journals/wjnf20

Isolation and Characterization of Nanofibrillated Cellulose from Sugarcane (*Saccharum officinarum*) Bagasse via Wet Disk Milling Mechanical Treatment

Asmaa Ali Mubarak , R.A. Ilyas , Faris M. AL-Oqla , Norzita Ngadi , Abu Hassan Nordin , M.F.M. Alkbir , Nadlene Razali , S.M. Sapuan , Mohd nor Faiz Norrrahim & Victor Feizal Knight

To cite this article: Asmaa Ali Mubarak , R.A. Ilyas , Faris M. AL-Oqla , Norzita Ngadi , Abu Hassan Nordin , M.F.M. Alkbir , Nadlene Razali , S.M. Sapuan , Mohd nor Faiz Norrrahim & Victor Feizal Knight (2026) Isolation and Characterization of Nanofibrillated Cellulose from Sugarcane (*Saccharum officinarum*) Bagasse via Wet Disk Milling Mechanical Treatment, Journal of Natural Fibers, 23:1, 2669376, DOI: 10.1080/15440478.2026.2669376

To link to this article: https://doi.org/10.1080/15440478.2026.2669376

Published online: 13 May 2026.

JOURNAL OF NATURAL FIBERS
2026, VOL. 23, NO. 1, 2669376
https://doi.org/10.1080/15440478.2026.2669376

Isolation and Characterization of Nanofibrillated Cellulose from Sugarcane (*Saccharum officinarum*) Bagasse via Wet Disk Milling Mechanical Treatment

Asmaa Ali Mubarak[a,b], R.A. Ilyas[a,c], Faris M. AL-Oqla[d], Norzita Ngadi[a], Abu Hassan Nordin[e], M.F.M. Alkbir[f,g], Nadlene Razali[h], S.M. Sapuan[i], Mohd nor Faiz Norrrahim[j], and Victor Feizal Knight[j]

[a]Faculty of Chemical and Energy Engineering, Universiti Teknologi Malaysia (UTM), Skudai, Malaysia; [b]Faculty of Science and Arts, Badr, University Zintan, Libya; [c]Centre for Advanced Composite Materials (CACM), Universiti Teknologi Malaysia (UTM), Skudai, Malaysia; [d]Department of Mechanical Engineering, Faculty of Engineering, The Hashemite University, Zarqa, Jordan; [e]Faculty of Applied Sciences, Universiti Teknologi MARA (UiTM), Arau Campus, Arau, Perlis, Malaysia; [f]Advanced Facilities Engineering Technology Research Cluster, Malaysian Institute of Industrial Technology (MITEC), Universiti Kuala Lumpur, Malaysia; [g]Plant Engineering Technology (PETech), UniKL Malaysian Institute of Industrial Technology (MITEC), Persiaran Sinaran Ilmu, Johor Darul Takzim, Malaysia; [h]Fakulti Teknologi dan Kejuruteraan Mekanikal, Universiti Teknikal Malaysia Melaka, Hang Tuah Jaya, Durian Tunggal, Melaka, Malaysia; [i]Advanced Engineering Materials and Composites Research Centre (AEMC), Department of Mechanical and Manufacturing Engineering, Universiti Putra Malaysia, UPM Serdang, Malaysia; [j]Research Centre for Chemical Defence, Defence Research Institute (DRI), Universiti Pertahanan Nasional Malaysia, Kuala Lumpur, Malaysia

ABSTRACT

Sugarcane bagasse fiber stands as a remarkable agro-waste plant, holding the key to unlocking its boundless potential as an abundant biomass source for an array of captivating biomaterial applications. In this study, the extraction of sugarcane bagasse nano-fibrillated cellulose (SCBNFC) involved two separate stages: delignification and mercerization to remove lignin and hemicellulose. Subsequently, the sugarcane bagasse cellulose fibers were subjected to further mechanical extraction using wet disc milling (WDM). In addition to TGA and XRD investigations, the materials were characterized using Fourier-transform infrared spectroscopy (FT-IR), Transmission electron microscopy (TEM), and point of zero charge (PZC). Significantly, SCBNFC all the cycles showed a high yield of around 99.9%, emphasizing that the fibers were fully developed into nanofibers through fibrillation. However, X-ray diffraction analyses indicated a subtle reduction in the crystallinity of the SCBNFC, with it decreasing from 56% to 57%. The ionized SCBNFC has promising prospects in nanocomposites, biopackaging, filtration, adsorbents, and others, hence encouraging research to discover and further develop this renewable nanomaterial for future green nanotechnology.

摘要

甘蔗渣纖維是一種極具價值的農業廢棄物，作為豐富的生物質來源，其蘊藏著無限潛力，可應用於多種引人注目的生物材料領域。本研究中，甘蔗渣納米纖維素(SCBNFC)的萃取過程包含兩個獨立階段: 脫木質化與絲光處理，用以去除木質素與半纖維素。隨後，將甘蔗渣纖維送入濕式圓盤研磨機 (WDM)進行進一步的機械提取。除熱重分析 (TGA)與X射線衍射 (XRD)研究外，亦採用傅立葉轉換紅外光譜 (FT-IR)、透射電子顯微鏡 (TEM)及零電荷點 (PZC)等方法對材料進行表徵。值得注意的是，所有週期的 SCBNFC 均展現出約 99.9% 的高產率，這強調了纖維已透過纖絲化完全發展為奈米纖維。然而，X 射線輻射衍射分析顯示 SCBNFC 的結晶度略有降低，從 56% 降至 57%。經離子化的 SCBNFC 在奈米複合材料、生物包裝、過濾、吸附劑等領域具有廣闊的前景，因此鼓勵研究人員發掘並進一步開發這種可再生奈米材料，以應用於未來的綠色奈米技術。

KEYWORDS

Nano fibrillated cellulose; Sugarcane bagasse fiber; delignification; mercerization; nano fibers; wet disk milling

關鍵詞

奈米纖維化纖維素; 甘蔗渣纖維; 脫木質素; 絲光處理; 奈米纖維; 濕式盤式研磨

CONTACT R.A. Ilyas ahmadilyas@utm.my Faculty of Chemical and Energy Engineering, Universiti Teknologi Malaysia (UTM), Skudai, Malaysia; Faris M. AL-Oqla Fmaloqla@hu.edu.jo Department of Mechanical Engineering, Faculty of Engineering, The Hashemite University, Jordan; Norzita Ngadi norzita@utm.my Faculty of Chemical and Energy Engineering, Universiti Teknologi Malaysia (UTM), Skudai, Malaysia; Mohd nor Faiz Norrrahim faiz@upnm.edu.my Research Centre for Chemical Defence, Defence Research Institute (DRI), Universiti Pertahanan Nasional Malaysia, Kuala Lumpur, Malaysia

Introduction

Cellulose is an important biopolymer that has many uses and is essential in our daily lives because of its unique properties. Cellulose is extensively utilized due to its biocompatibility, biodegradability, abundant availability, and sustainability. Typically, cellulose fibers consist of aggregates of nanofibers with diameters between 5 and 70 nm, and lengths ranging from 100 nm to several micrometers (Ilyas Rushdana et al. 2017; Sapuan, Lamin Sanyang, and Ridzwan Ishak 2016). These nanofibers, designated by many names depending on their source and quality, can be extracted from a variety of natural materials, such as kenaf (Ilyas et al. 2019), softwood wood (Li et al. 2018), cotton (Sun et al. 2021), wheat straw (Sihag, Sheetal, and Pal 2022), rice straw (Oun and Rhim 2018), coir fiber (Fernandes et al. 2023), sugarcane bagasse and banana peels (Pelissari et al. 2017a), pinecones (Jackpine: Pinus banksiana Lamb), potato tuber cells (Mehanny et al. 2021), carrot (Guimarães et al. 2016), eucalyptus, and pine fibers (Ilyas et al. 2019), corn husk and oat hulls (Valdebenito et al. 2017) and bamboo fiber (Llanos and Tadini 2018; Xie et al. 2016) among cited sources. Due to their distinctive physical properties, these nanofibers have attracted significant interest from researchers over the past few decades. They are characterized by high crystallinity, a large surface area, a high aspect ratio, and abundant surface hydroxyl groups. Additionally, they exhibit favorable thermal properties, including a low coefficient of thermal expansion and strong thermal resistance. Their exceptional mechanical properties, such as high specific strength, stiffness, and modulus, further enhance their appeal. Moreover, the production of these nanofibers is cost-effective and environmentally friendly, making them a versatile nanomaterial with a wide range of potential applications (Ilyas et al. 2019).

Nanocellulose has gained considerable recognition as an environmentally friendly and sustainable material owing to its outstanding properties, including high aspect ratio (Nguyen et al. 2021), large specific surface area (Syafri et al. 2022a), superior mechanical strength, biocompatibility, and renewability (Dai et al. 2020; K. Zhang et al. 2018). The abundance of hydroxyl functional groups on its surface enables diverse chemical modifications, facilitating the development of advanced functional materials (Hu et al. 2024; Phanthong et al. 2018). Nanocellulose is generally classified into bacterial nanocellulose (BNC), cellulose nanocrystals (CNCs), and cellulose nanofibrils (CNFs), with their morphology and physicochemical properties strongly dependent on the cellulose source, extraction routes, and processing conditions (Gan et al. 2020). Among these, CNFs have attracted particular interest due to their high durability and potential applications in papermaking, food packaging, and emerging energy technologies such as supercapacitors, lithium-ion batteries, and triboelectric nanogenerators (Xing et al. 2019; H. Zhang et al. 2019). However, improving the thermal stability of CNFs, which typically degrade between 200°C and 350°C, remains a key challenge for their broader industrial utilization (Lu et al. 2020).

Nanocellulose exhibits low density, high dimensional stability, low thermal expansion, and tunable surface chemistry, making it an excellent-reinforcing material for polymer composites (Abral et al. 2021; Gan et al. 2020). Consequently, its properties are strongly influenced by raw material sources, pretreatment strategies, and isolation processes (Imraan et al. 2023; Nazrin et al. 2021; Reshmy et al. 2020). CNFs are typically produced through mechanical disintegration processes that involve intense shear and impact forces, resulting in the progressive breakdown of cellulose fibers into nanoscale fibrils via a top – down approach (Q. Q. Wang et al. 2012; S. Zhang et al. 2022). The efficiency of CNF production and the resulting fibril morphology are significantly affected by the selection of milling techniques (e.g., refining, microfluidization, grinding, ball milling, cryo-crushing, and ultrasonication), operational parameters (milling cycles, speed, temperature, and solid concentration), and the use of milling additives or pretreatments. Milling additives such as water, dispersing agents, surfactants, or chemical pretreatments can reduce fiber aggregation and energy consumption, thereby enhancing fibrillation efficiency and controlling nanocellulose structure. These factors play a crucial role in determining the crystallinity, aspect ratio, surface chemistry, and overall structural characteristics of CNFs (Norfarhana et al. 2024).

Wet disc milling (WDM) has recently gained increasing attention due to its high energy efficiency and effective fiber fibrillation capability (Yasim-Anuar et al. 2020a). For instance, CNFs extracted from wastepaper using WDM exhibited a reduction in fiber diameter from the micrometer scale to 20–40 nm after 10 milling cycles (Shirani et al. 2022). Moreover, the incorporation of CNFs significantly enhanced the tensile strength and Young's modulus of poly(R)-3-hydroxybutyrate-co-(R)-3-hydroxyhexanoate

(PHBHHx), with improvements of 19% and 12%, respectively, compared to the neat polymer (Y. Wang et al. 2025).

Scientifically known as *Saccharum officinarum*, sugarcane is a primary source of sugar production that is of global importance (Anitha et al. 2024). Beyond its traditional use, sugarcane is being recognized more and more for its adaptability in producing nanocellulose, a substance with a broad range of uses in a variety of industries, such as packaging, electronics, and biomedicine (Abdel-Hakim and Mourad 2023). Sugarcane-derived nanocellulose possesses exceptional characteristics, including superior strength, biodegradability, and biocompatibility. Consequently, it emerges as an attractive substitute for conventional materials in the pursuit of sustainable development (Abdullah et al. 2021).

This work successfully isolated NFCs from SCB using wet disc milling. A comprehensive assessment of the structural and physicochemical properties of sugarcane bagasse fibers was conducted using a variety of techniques, including FT-IR spectroscopy, TEM, zeta potential analysis, and X-ray diffraction (XRD). Moreover, we used thermogravimetric analysis (TGA) to assess the thermal characteristics.

Materials and methods

Materials

The sugarcane bagasse fibers used in this investigation were obtained from the Johor Bahru municipality in Malaysia. A variety of chemical reagents were used in the experiments. QRëc supplied 99% pure sodium hydroxide (NaOH), Sigma supplied 80% pure sodium chlorite ($NaClO_2$), and QRëc provided 99.8% pure acetic acid (CH_3COOH).

Extraction of cellulose

In this investigation, cellulose fibers were isolated from SCB using recognized techniques for delignification and mercerization (Asmaa Ali Mubarak et al. 2024; Ilyas et al. 2017). The extraction procedure began by mixing 5 g of powdered and dried SCB with a solution of sodium chlorite that was 200 mL in volume and had 20 different concentrations of sodium chlorite. Next, a magnetic stirrer was employed to continuously swirl this mixture at 75°C for 3.5 h. Filter paper filtering was then used to recover the solid residue that included hemicellulose. Following that, a 200-mL NaOH 5% w/v solution was added to the hemicellulose mixture and agitated for 2 h. To obtain the cellulose residue, another round of filtration was performed. NaOH was employed to keep the sample's pH at 7.5. Following an extra filtration stage, the leftover cellulose particles, known as SCBC, were correctly measured before being dried overnight at 75°C to ensure full moisture removal, as shown in Figure 1.

SCBNFC Extraction

The wet disk milling (WDM) process was employed using cycles 5, 10, 15, and 20 to convert cellulose into nano-sized fibrils following purification. The procedure depicted in Figure 1 was utilized to generate nano-fibrillated cellulose from sugarcane bagasse, referred to as SCBNFC. Grow Engineering of Adachi-ku, Tokyo, Japan, manufactured the high-shear ultrafine friction grinder that was utilized for the WDM process. Before grinding, SCBC was immersed in distilled water for 72 h. Two liters of 2 wt% fiber suspension were added to the grinder and rotated at 1800 rpm. This process produces fibers known as sugarcane bagasse nano-fibrillated cellulose (SCBNFC). We kept the SCBNFC slurry at 2°C in a sealed jar to preserve it for later use. To enable additional investigation, a 10 mL sample of the slurry was freeze-dried. Ecological delignification and mercerization, combined with WDM, created SCBNFC with unique properties appropriate for a range of uses.

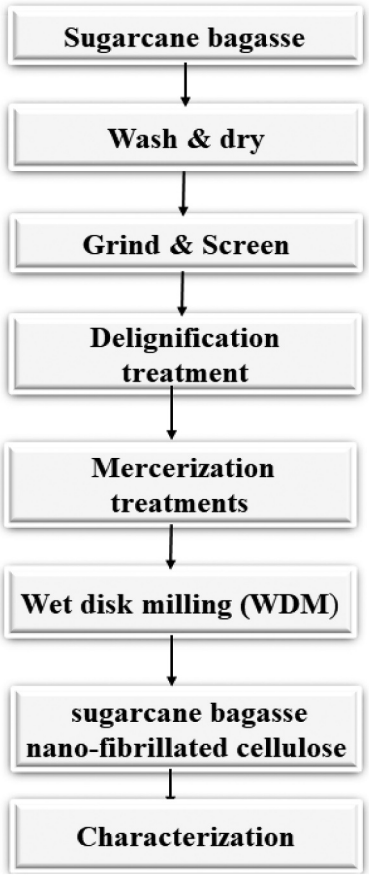

Figure 1. Schematic illustration of SCBNFC isolation.

Characterization

SCBNFC yield

To begin the process, a 2 wt% solution was prepared and then diluted with distilled water. The mixture was centrifuged at 4500 rpm for 20 min, resulting in nano-fibrillated material collecting in the supernatant, while non-fibrillated and partially fibrillated components settled as sediment. The separated compounds were dried in a halogen desiccator at 90°C until a constant weight was achieved. Finally, the yield was calculated using Equation (1).

$$yield(\%) = (1 - \frac{\text{weight of dried sediment}}{\text{weight of diluted sample} \times \%\ \text{Sc}}\ \text{x}\ 100$$

where Sc (%) is the percentage of materials. The results are shown as the mean values from three different experiments.

Chemical makeups

As reported by (Arisyah et al. 2017) The chemical composition of the starting material was analyzed using gravimetric methods to quantify lignin, cellulose, and hemicellulose on a dry basis. Sugarcane bagasse (SCB) was immersed in a 5% (w/v) sodium chlorite ($NaClO_2$) solution at 70°C for 90 min, with the pH maintained between 4 and 5. After treatment, the samples were dried in an oven for 24 h and then cooled in a desiccator until they reached a stable weight (Arisyah et al. 2017). The weight loss observed after treatment was attributed to the lignin content, while the remaining weight represented holocellulose, which includes both hemicellulose and cellulose. To isolate cellulose, holocellulose was rinsed with deionized water and then treated with a 6% (w/v) potassium hydroxide (KOH) solution at 25°C for 24 h to remove hemicellulose.

After the treatment, the samples were dried in an oven for 24 h and then cooled in a desiccator before analysis. The final weight was used to determine the cellulose content.

Functional group profile

The functional groups in the samples were analyzed using the PerkinElmer 2000 Spectrum GX model instrument. For the analysis, 2 mg of the sample was mixed with potassium bromide (KBr) to reach a total weight of 200 mg. The instrument operated with a precision of 4 cm^{-1}, measuring wavelengths from 400 cm^{-1} to 4000 cm^{-1} at a scanning speed of 20 kHz.

Degree of crystallinity

XRD analysis was performed using a Bruker Advance D8 apparatus (Germany). Measurements were taken across a 2θ range with 0.02° increments, while maintaining a temperature range of 5°C to 40°C. The crystallinity index (CrI) was calculated using Equation (2), as reported by (Segal, Creely, and Martin 1952).

$$Crl(\%) = \left(\frac{I002 - Iam}{I002}\right) \tag{2}$$

Significant variables in the analysis are the amplitude of the reflection on the plane (200) (2θ = 21–23°), known as I_{002}, and the intensity of the amorphous cellulose component (2θ = 18°), known as I_{am}.

Surface morphology

Transmission electron microscopy (TEM) was employed to observe the nanostructural morphology of the SCBNFC. The analysis was performed using a Philips Tecnai 20 TEM operated at an accelerating voltage of 200 kV and equipped with a standard inclined sample holder. Prior to imaging, the SCBNFC suspension was prepared by ultrasonically dispersing the particles in distilled water for 10 min to ensure adequate individualization of the nanofibres. A drop of the diluted suspension was then carefully deposited onto a carbon-coated copper grid and allowed to dry at room temperature.

Point zero charge (PZC)

To determine the point of zero charge (PZC) of SCBNFC, a series of analytical preparations were conducted. First, 250 mL of a 0.1 M NaCl solution was added to each of five Erlenmeyer flasks. The pH of these solutions was then adjusted from 2 to 10 using 0.1 M HCl and 0.1 M NaOH. After adjusting the pH, 5 g of SCBNFC were added to each flask. The samples were left undisturbed for 48 h, after which the final pH of each solution was recorded. The pH at which the system exhibited the most favorable activity was identified as the PZC. Equation (3) was used for the final calculation of pHPZC based on the most recent analysis.

$$\Delta pH = pH_1 - pH_2 \tag{3}$$

The pH values before and after the experiment are represented by the numbers pH_1 and PH_2, respectively. The intersection points of the pH vs. pH plot that indicate pH_{PZC} are those where pH = 0.

Thermogravimetric analysis (TGA)

This approach demonstrates the overall effects of temperature on weight loss. The Thermogravimetric Analysis (TGA) provides a comprehensive insight into the degradation patterns of SCBNFC. The thermal stability of SCBNFC was determined by submitting it to various treatments and monitoring its response with a PerkinElmer TGA 4000 thermogravimetric analyzer calibrated in the United States. The device is designed to handle small sample sizes effectively, providing accurate measurements within this range of a typical sample mass is around 5–10 mg. Aluminum pans were used in experimental methods under a nitrogen atmosphere. The temperatures ranged from 25°C to 800°C, with a heating rate of 10°C per minute.

Results and discussion

SCBNFC yield

Figure 2 illustrates the yield of SCBNFC isolated from sugarcane bagasse fiber under various processing conditions, with the number of WDM cycles set at 5, 10, 15, and 20. The results reveal that SCBNFC-20 yielded the lowest amount at 98.4%. In contrast, the yields for SCBNFC-5, SCBNFC-10, and SCBNFC-15 were slightly higher, measuring 99.3%, 99.5%, and 99.06%, respectively. This represents incremental increases of 0.3%, 0.2%, and 0.3%. Overall, with a final yield of 99.6 wt%, the CNF extraction process demonstrates promising efficiency and potential for further applications.

Table 1 provides the reported synthesizing requirements of the SNPC and the related features when compared to different types of lignocellulosic biomasses. With WDM, mechanical defibrillation of cellulose fibers may be achieved with great precision, leading to a significant increase in SCBNFC production through NFC synthesis. Nanofibers undergo a transformation when subjected to WDM treatment, which increases their wet strength and shear stresses (Norfarhana et al. 2024). The yield of cellulose nanofibers is typically low during the TEMPO oxidation process of wood fibers. Based on this, the recent study has shown a yield of over 30%, which is high. The (Masruchin et al. 2020) study reports a yield of 46%, while the (Jonasson et al. 2020) study has a yield range of 44–55%. This work demonstrates a significantly greater production of NFC from sugarcane bagasse fiber (SCBF) compared to earlier studies conducted by (Ilyas et al. 2019; Ilyas, Sapuan, and Ishak 2018). In their research, they were able to synthesize 29% of SPF nanocrystalline cellulose using a chemical procedure that involved acid treatment at 60°C and alkali

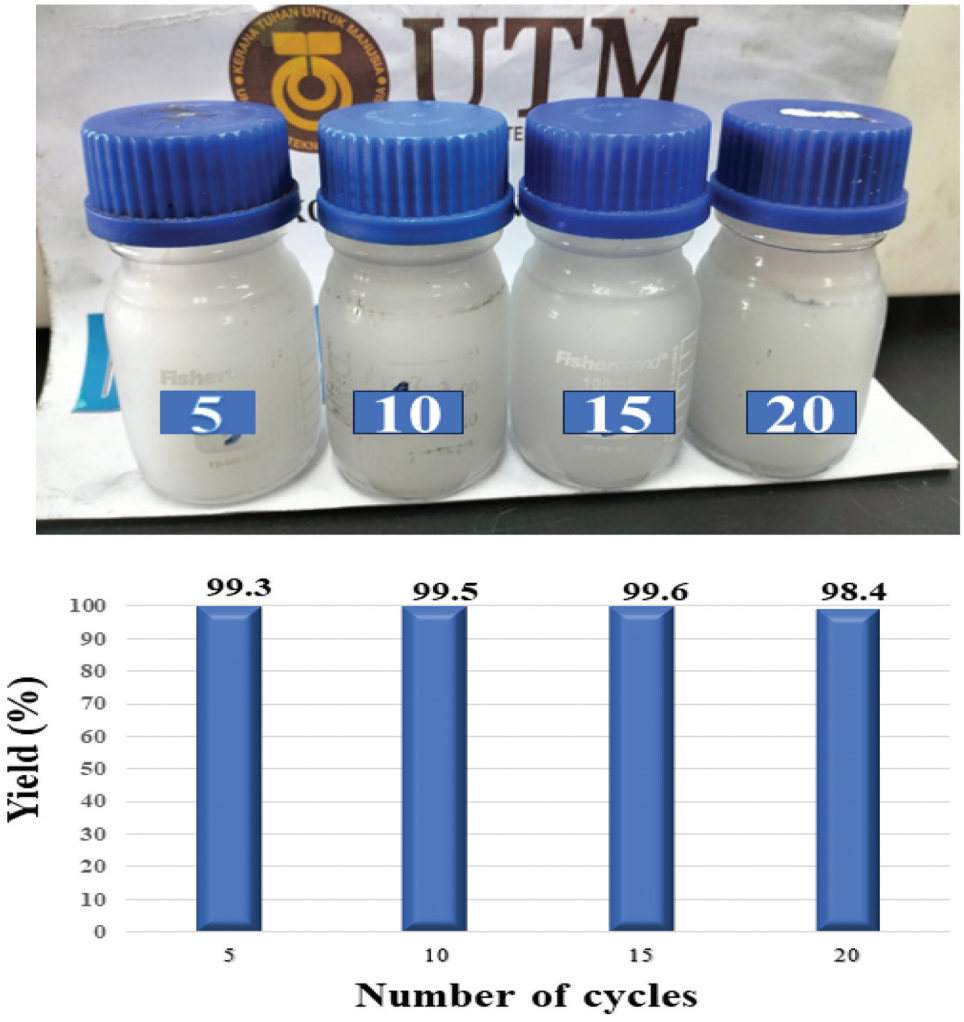

Figure 2. Yields of attained nanofibers after several cycles.

Table 1. Comparison of the morphological, physicochemical, and thermal of SCBNFC with other common lignocellulosic fibers.

		Morphological properties		Chemical properties	Physical properties	Thermal properties maximum	
Lignocellulosic biomass	Extraction method	Shape	Diameter (nm)	Cellulose yield (wt%)	CrI (wt%)	(Tm, ◦C)	Ref.
Jack fruit peduncle	–Acidified chlorination –Alkalization treatment –Acid hydrolysis	Cylindrical structure	27300	82.00	79.5	349	Devarajan et al. (2024)
Red banana empty fruit bunches	– Alkaline treatment - $NaClO_2$ bleaching - Ball mill treatment	Web-like structure	15–35	45.00	69.5	421	Rajan et al. (2023)
Millet husk	– Alkaline treatment - ($NaOH + H_2O_2$) bleaching - Steam explosion - Acid hydrolisis + homogenization treatment	Web-like arrangement	10–12	65–70	58.45	341	Midhun Dominic et al. (2022)
Cuscuta reflexa	– Alkaline treatment –Steam explosion treatment	Thread network structure	10–30	78	67	363	Dominic, C.D et al. (2020)
Sunn hemp	– Alkaline treatment –DMSO treatment –Acid hydrolysis treatment	Web-like structure	55 ± 13	94.83	72.52	–	Mahur et al. (2023)
Agave gigantea	– Alkaline treatment -($NaOH + CH_3COOH + NaClO_2$) bleaching –Ultragrinding+ ultrasonication treatment	Fibril-fibril structure	4.07		65.21	355.91	Syafri et al. (2022b)
Sugarcane bagasse	– Alkaline treatment –Acid treatment –Alkaline treatment –High-speed grinding	Spherical/rod like structure	57.07	65.00	58.32	–	Gond, Gupta, and Jawaid (2021)
Rice husk	– Alkaline treatment -H_2O_2 bleaching – HPH treatment	Fiber networks	10.15–12.42	23.54	62–72	>380	Samsalee, Meerasri, and Sothornvit (2023)
Timoho fiber	– $NaClO_2$ bleaching –Alkaline treatment –Acid hydrolysis	Glycosidic network	68.94 ± 8.36	84.75	71.14	365.36	Diharjo et al. (2023)
Wheat straw	-(CH_3COOH+ $NaClO_2$) bleaching – Alkaline treatment –Grinding treatment	Cylindrical	35	–	–	–	Kumar Trivedi, Kumar, and Gupta (2023)
Dunchi fiber	– Alkaline treatment -(H_2O_2+tetra-acetyl ethylene diamine, TAED) bleaching – ($CH_3COOH + HNO_3$) bleaching – Acid hydrolysis	Needles	20.67 ± 7.39	–	66.7	360	Khan et al. (2020)
Palm wastes	– Alkaline treatment – Acid hydrolysis	Sphericles	42–82	–	27	–	Mehanny et al. (2021)
Sugar palm fiber	– ILs pretreatment – H_2O_2 bleaching – WDM treatment	Thread-like structure	3.30 ± 0.68	96.89	61.62	360.5	Norfarhana et al. (2024)
Sugarcane bagasse fiber	–delignification and mercerization treatment –WDM treatment	Thread-like structure	12.32 ± 2.37	99.6	57.87	360	**Current study**

treatment at 90°C. Subsequently, the material should undergo mechanical fibrillation to achieve a concentration of 52% by weight of solid particles in the form of SPF nano fibrillated cellulose, using a high-pressure method.

Chemical compositions

The chemicals that make up natural fibers greatly affect their mechanical, heat, and physical properties. Amorphous lignin and a hemicellulose-reinforced structure of crystalline cellulose microfibrils make up most plant fibers (Ismail, Akpan, and Dhakal 2022). However, the exact morphology of these compounds changes based on origin, the temperature, the soil, age, and how they are processed (Ilyas et al. 2017). The chemical composition of raw SCB and SCBC was analyzed to gain insights into the properties of the natural fibers. The results, presented in Table 2, demonstrate that the extraction process using $NaClO_2$ and NaOH significantly altered the morphology of sugarcane bagasse. During the whitening step, this process removed hemicellulose, silica, soluble mineral salts, and ash from the raw fibers, resulting in purified cellulose (Asmaa Ali Mubarak et al. 2024; Dufresne et al. 2000; Sheltami et al. 2012). Temperature and pH play a crucial role in this process. Typically, reactions proceed more quickly at higher temperatures and elevated pH levels. In the second stage, chemical treatment further degrades and eliminates additional fiber components, thereby improving the material's properties.

Table 2 displays the chemical composition of SCB fibers following various treatment stages. Raw SCB fibers contain approximately 46% cellulose, 16% hemicellulose, and 38% lignin. In contrast, treated SCBC has a composition of 84% cellulose and 22.5% hemicellulose. This increase in cellulose content (from 46% in raw fibers to 84% in SCBC) demonstrates the effective removal of lignin and other components during the delignification and mercerization processes, which likely facilitated the separation of insoluble compounds in the treated fibers (Asmaa Ali Mubarak et al. 2024). Because of this, SCBC is the best fiber for making nanofibrillated cellulose through mechanical treatment in a wet disc mill because it has the best makeup and properties.

Functional group profile

FTIR spectroscopy is employed to characterize the chemical composition and identify both amorphous and crystalline structures in nanofibers (Mayerberger et al. 2018). Figure 3 presents the typical FTIR spectra for SCBNFC-5, 10, 15, and 20, with detailed vibrational IR assignments listed in Table 3. The spectra of all samples exhibit nearly identical features, indicating a consistent chemical composition across these nanofiber samples. Similar findings were reported by Fahma and Ilyes, who studied nanofibers derived from OPEFB and SPF using varying concentrations of H_2SO_4, different HPH passes, and pressure conditions (Fahma et al. 2010).

Bands at 3420, 2930, 1430, 1370, and 890 cm^{-1} in the spectra are ascribed to cellulose I (He et al. 2022). The peak at 3400–3500 cm^{-1} indicates cellulose OH bond stretching, while the band at 2900 cm^{-1} indicates CH_2 bond stretching (Rana and De la Hoz Siegler 2023). The peak at 1645 cm^{-1} in all samples may be due to cellulose absorbing water. This band is formed by water molecules bending due to cellulose's water resistance (Fahma et al. 2010; He et al. 2022; Rana and De la Hoz Siegler 2023). (Mayerberger et al. 2018) attributed the high absorption band at 1428–1433 cm^{-1} to inter-molecule hydrogen bonding at the C_6 group.

The bending vibrations of the C–H and C=O groups within the aromatic rings of polysaccharides are responsible for the peak found in the spectra of all samples between 1330–1369 cm^{-1}. Furthermore, Haafiz et al. (2014) reported similar findings for cellulose nano whiskers from microcrystalline cellulose nanofibers in oil palm waste. Furthermore, nanocellulose from SCB gave comparable outcomes (Mandal and

Table 2. Chemical composition of SCB and SCBC.

Sample	Cellulose (%)	Hemicellulose (%)	Lignin (%)
Raw SCB	46	16	38
SCBC	84	22.5	–

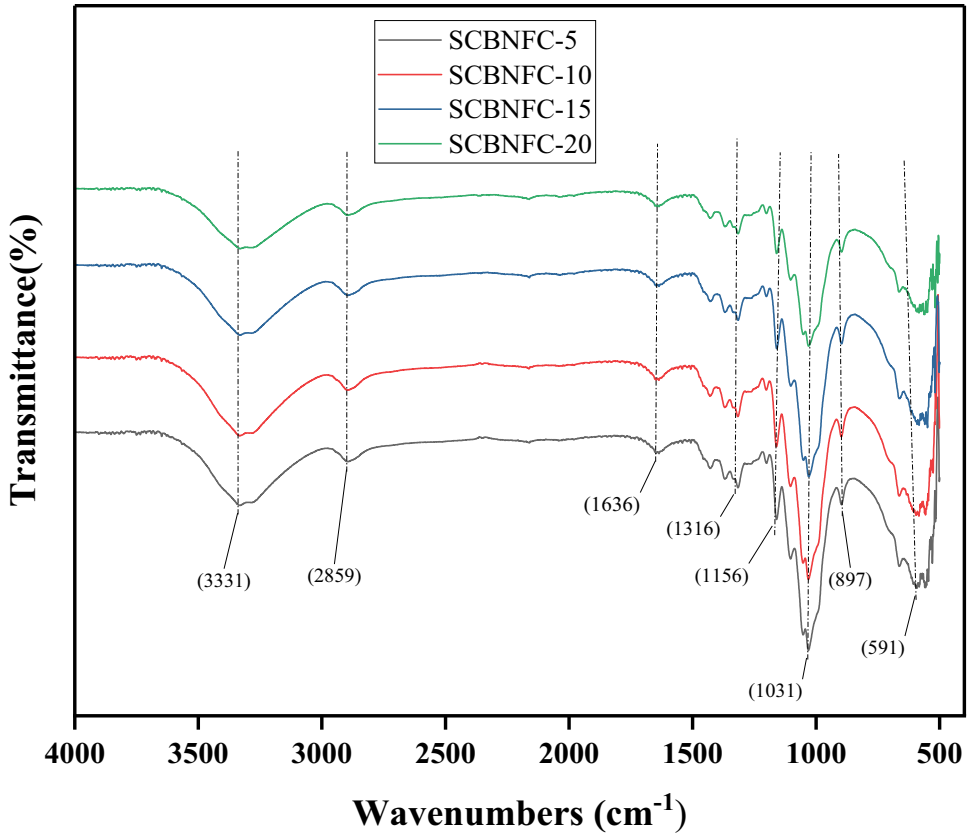

Figure 3. FTIR spectra of sugarcane base samples.

Table 3. Result of FTIR spectra for the samples.

	wavenumber (cm^{-1})			
Peak Assignment	SCBNFC-5	SCBNFC-10	SCBNFC-15	SCBNFC-20
OH groups	3331.05	3330.90	3330.50	3332.10
CH_2 groups	2895.46	2894.85	2895.13	2895.53
C = O stretch	1636.06	1635.89	1635.98	1635.80
CH_2 bending	1428.20	1428.50	1428.65	1428.77
C-H asymmetric stretch	1316.06	1316.08	1316.02	1315.97
C-O-C stretch	1159.99	1159.81	1159.27	1159.93
CH-H	897.15	896.65	896.65	897.00

Chakrabarty 2011). Bands at 1163–1167 cm^{-1} suggest the presence of C–C bonds. The C–O–C glycosidic ether band at 1105 cm^{-1}, which decreased in CNF probably due to WDM treatment, indicating a reduction in molecular weight. Furthermore, the C-H rocking vibration indicative of anomeric vibration of β-glucosides is associated with the peak observed at 894–896 cm^{-1}, consistent with (Norfarhana et al. 2024).

Degree of crystallinity

The crystallinity of the synthesized cellulose was evaluated using X-ray diffractograms. The XRD patterns of the SCBNFC synthesized at distinct WDM cycles in this study are depicted in Figure 4. The discernible diffraction peak observed at a consistent region around 2θ = 22.28–22.44° in all samples is characteristic of cellulose Iβ structure, effectively illustrating the crystalline arrangement of cellulose (Souza et al. 2020). Subsequently, a significant splitting peak can be seen at 2θ = 27°, suggesting a certain amount of cellulose II phase development (Del Cerro et al. 2020), and the XRD pattern of SCBNFC is consistent with the findings of (Ramki et al. 2019). The findings show that crystallinity is more effectively extracted from SCB following WDM treatment. Table 4 presents a comprehensive list of CrI values associated with all WDM cycles of

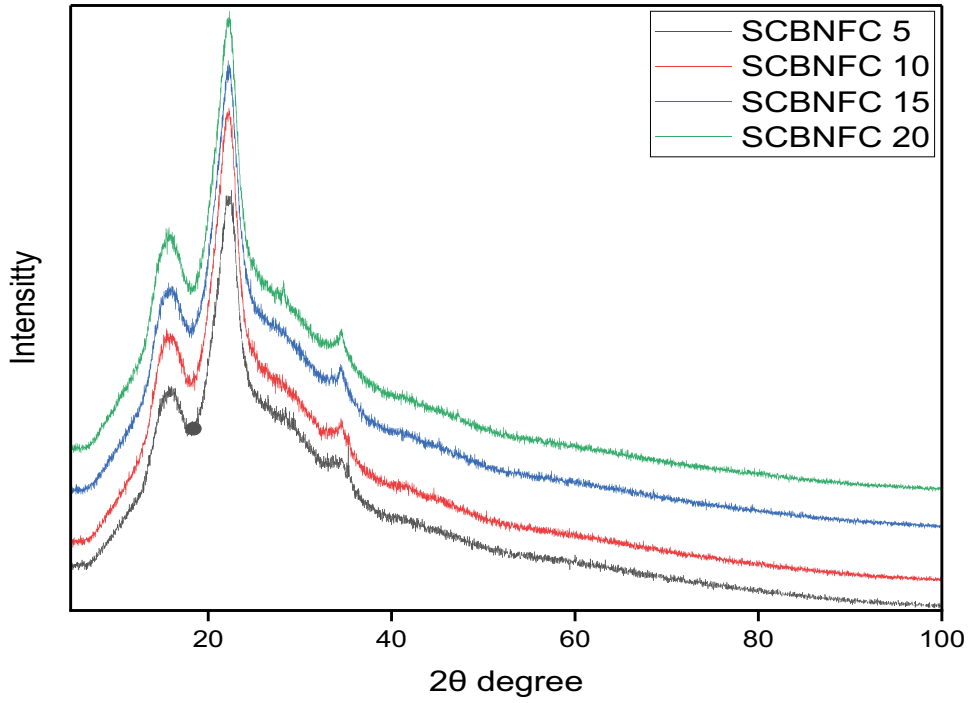

Figure 4. X-ray diffraction patterns for SCB samples.

Table 4. Summary of XRD data for the SCB samples.

Sample	I_{002}	I_{am}	X_c%
SCBNFC-5	5715	2478	56.64
SCBNFC-10	6460	2721	57.87
SCBNFC-15	6382	2715	57.45
SCBNFC-20	6532	2813	56.93

SCBNFC samples. By the second and third cycle of WDM, the CrI of cellulose fibers was approximately 57.87% and 57.45 respectively. The CrI values for SCBNFC5, and SCBNFC20 decreased slowly to 56.64%, and 56.93%, respectively. Intense mechanical stresses including high shear and friction applied during WDM may degrade the crystalline structure of NFC, resulting in lower CrI values (Norrrahim et al. 2018). A discernible pattern can be experienced where in the crystallinity of SCBNFC decreases as the number of milling cycles increases gradually. A similar pattern of findings was observed in the isolation of cellulose nanofiber from oil palm mesocarp fiber, as determined by (Norrrahim et al. 2019). According to (Yasim-Anuar et al. 2020c), this phenomenon can be elucidated by the disturbance occurring within the cellulose crystalline region due to the nano-fibrillation process induced by WDM, leading to a reduction in overall crystallinity. Additionally, this occurrence might be attributed to the shear force intensity of the mechanical treatment, inducing molecular motion with cellulose, thereby initiating the deconstruction of cellulose crystals, as reported by (Supian et al. 2020).

The relatively small differences observed among SCBNFC samples processed at different WDM cycles can be interpreted by considering the inherently progressive yet asymptotically saturating behavior of mechanical fibrillation processes in lignocellulosic systems. During the initial milling cycles, the combined delignification and mercerization pretreatments significantly weaken the supramolecular architecture of the cellulose fiber wall, particularly through the removal of residual lignin and hemicellulose components and the disruption of the extensive hydrogen-bonding network that stabilizes the hierarchical microfibrillar structure. This pretreatment-induced loosening of the interfibrillar matrix facilitates rapid mechanical delamination during early WDM cycles, thereby enabling the cellulose bundles to be efficiently disintegrated into nanoscale fibrillar structures with relatively limited energy input. Consequently, a substantial proportion of the fibrillation process is completed during the first few milling cycles, which explains why subsequent cycles produce only modest variations in structural characteristics. Such behavior is consistent

with observations reported for mechanically produced cellulose nanofibrils, where the efficiency of fibrillation increases dramatically after chemical pretreatment due to reduced fiber cohesion and improved accessibility of shear forces to the microfibrillar interfaces (Pelissari et al. 2017b; Tonoli et al. 2007). Moreover, once a large fraction of the fiber population has already transitioned into individualized nanofibrils, additional mechanical treatment predominantly acts on already fibrillated structures rather than intact fibers, thereby limiting the magnitude of observable physicochemical changes. As a result, key material parameters such as yield, crystallinity index, and thermal stability exhibit only marginal variation across increasing WDM cycles, indicating that the fibrillation process progressively approaches a structural equilibrium state. Similar saturation trends have been documented in recent nanocellulose production studies, where the transition from fiber fragmentation to fibril refinement marks the onset of diminishing returns in mechanical processing efficiency (Guélon, Mathias, and Stoodley 2011; Ning et al. 2019; Yasim-Anuar et al. 2020b).

From a structural perspective, the minor reductions in crystallinity and subtle shifts in thermal degradation behavior observed at higher milling cycles can be attributed primarily to localized mechanical damage within the crystalline domains rather than extensive degradation of the cellulose polymer framework (de Santana et al. 2024; Hassan et al. 2012). Repeated shear and impact forces generated during prolonged mechanical milling can induce partial disruption of ordered cellulose I crystallites, leading to slight decreases in crystallinity as well as limited cellulose chain scission events within the amorphous–crystalline interfacial regions. However, because the majority of cellulose crystallites remain structurally intact, these alterations manifest only as small variations in thermal stability parameters rather than significant changes in degradation pathways. Recent high-resolution structural analyses of mechanically fibrillated nanocellulose have similarly demonstrated that extended mechanical treatment tends to generate surface fibrillation, increased fibril flexibility, and minor crystalline distortion without fundamentally altering the overall crystalline polymorph of cellulose (Elsayed et al. 2023). In this context, the slight decrease in crystallinity at higher WDM cycles may also reflect the formation of highly individualized nanofibrils with increased surface disorder, which inherently contributes to a modest reduction in the proportion of ordered crystalline regions (Ning et al. 2019; Yasim-Anuar et al. 2020b). Importantly, such structural changes do not necessarily indicate material deterioration but may instead improve the surface reactivity and interfacial compatibility of nanocellulose in composite systems. Consequently, the observed saturation behavior suggests that an optimal balance between fibrillation efficiency and structural preservation is achieved at relatively moderate milling cycles, beyond which further mechanical processing provides diminishing structural benefits while potentially increasing energy consumption. This interpretation aligns with recent process optimization studies indicating that excessive mechanical treatment rarely improves nanocellulose properties once full fibrillation has been achieved and may instead lead to unnecessary energy expenditure during large-scale production (Guélon, Mathias, and Stoodley 2011; Tsade, Anshebo, and Sabir 2021).

The high crystallinity index (CrI) observed (approximately 57%) suggests that SCBNFC can serve as a potent reinforcing phase in polymer matrices. The interpretation of the XRD data reveals that while mechanical shear induces minor surface disorder, the crystalline core remains robust, facilitating efficient stress transfer across the fiber–matrix interface. This structural integrity, coupled with the potential for silanization or acetylation, can be exploited to overcome the inherent hydrophilicity of cellulose, thus improving compatibility with hydrophobic industrial polymers.

A critical finding of this research is the determination of the Point of Zero Charge (PZC), which provides a fundamental baseline for the material's application in environmental remediation. By understanding the surface charge behavior, SCBNFC can be strategically functionalized with amino or carboxyl groups to target specific heavy metal ions or organic dyes in wastewater. The synthesized nanofibers' high yield (99.6%) and thermal stability up to 360°C position them as a sustainable and cost-effective alternative to synthetic adsorbents, capable of withstanding the rigorous conditions of industrial filtration cycles.

The biocompatibility and biodegradability inherent to *Saccharum officinarum* derivatives, combined with the thread-like morphology observed in TEM imaging, suggest significant potential in the development of antimicrobial food packaging and biomedical scaffolds. The high surface reactivity of the ionized SCBNFC allows for the grafting of bioactive molecules or the incorporation of silver nanoparticles, creating active materials that do not merely contain products but interact with the environment to extend shelf-life or facilitate tissue regeneration.

Surface morphology

The length, shape, and degree of nano crystallization of NFC have an impact on their structure and reinforcing characteristics (Ilyas et al. 2019). The aggregated nanofibers, which are connected by many intermolecular and intramolecular hydrogen bonds, need to undergo mechanical processing to obtain a uniform NFC without affecting its natural structure (Potthast et al. 2022). The shape and microstructural properties of selected SCBNFC films were analyzed using TEM images (Figure 5). During the process of

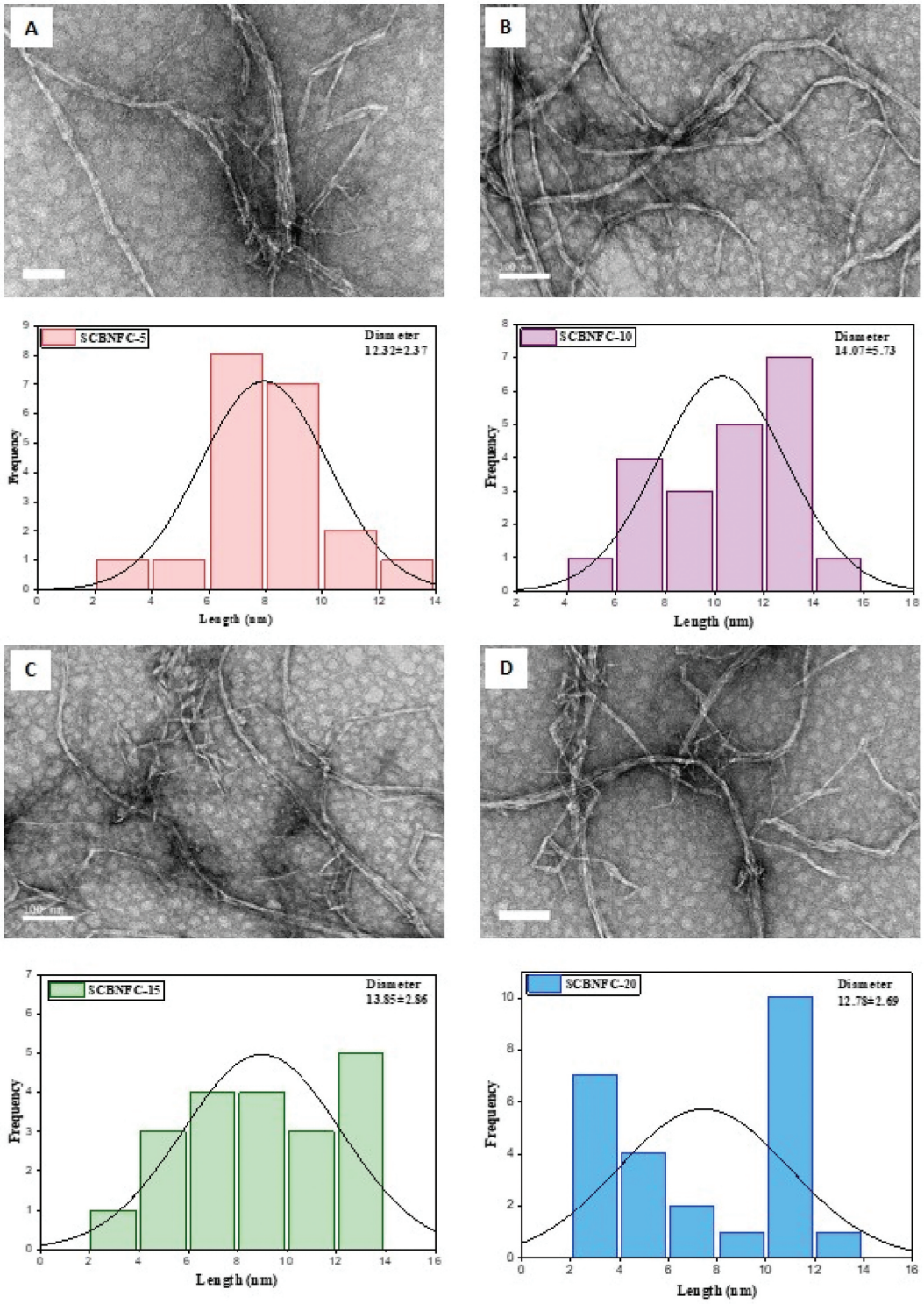

Figure 5. TEM profile of SCBNFC-5 (A), SCBNFC-10 (B), SCBNFC-15 (C), and SCBNFC-20 (D).

mechanical refinement, the surfaces of fibers experience shearing action which causes the extraction of microfibrils from the cell wall (Ilyas et al. 2021). TEM images reveal that SCBC, when processed with WDM, displays an irregular structure indicative of nanofibrillation This effect results from the placement of millstones prior to WDM treatment, generating significant shearing and frictional forces on the outer layer of the cellulose fibers. Instead of being processed with grinding disks, the fibers experience substantial impact and frictional forces through this method, leading to effective fibrillation (Taflick et al. 2017). The diameter values of NFC that were separated from sugarcane bagasse using WDM are as follows: The diameters of the SCBNFC-5, SCBNFC-10, SCBNFC-15, and SCBNFC-20 are 12.32 ± 2.37 nm, 14.07 ± 5.73 nm, 13.85 ± 2.86 nm, and 12.78 ± 2.69 nm, respectively. This outcome is described in Table 5. The microscopic drawing displays for BNFC a tangled structure and single fibers that indicate the fibrillation process during the mechanical process of WDM, due to the rotating disk creating high shear forces that act on the fibers, pulling them apart longitudinally. This impact force helps to break down the fiber bundles further. The presence of water in the milling process aids in the separation of fibers by reducing friction, and the hydrodynamic forces also help to transport the fibers through the milling chamber effectively. The reported diameters of NFC generated after IL pretreatment, H_2O_2 bleaching, and WDM treatment for SPF are slightly greater than the values of 3.30 ± 0.68 nm reported by Norfarhana et al. (Norfarhana et al. 2024). Nevertheless, they are somewhat smaller than the 6–22 nm sizes documented for NFC generated through different methods using bleached sugarcane bagasse pulp. In addition, Pelissari et al. (Potthast et al. 2022) documented that the diameter of NFC from sugarcane bagasse is 31 ± 10 nm.

Point zero charge (pH_{pzc})

The point of zero charge (pHPZC) is defined as the pH level at which a solid's surface has no net electric charge, resulting from an equal density of positive and negative charges. This parameter is specific to the interaction between an electrolyte or aqueous solution and a particular surface. Predicting surface functional group ionization and their interactions with insoluble species requires an understanding of pH_{PZC}. Following Elsayed et al. 2023, the surface acquires a positive charge at pH values below the pH_{PZC} and a negative charge at pH values above the pH_{PZC}.

The pH_{PZC} of SCBNFC for each cycle is 6.3, as illustrated in Figure 6 It is reasonable to conclude from this pattern that the adsorbent surface is negatively charged at pH levels above 6.3 and positively charged at pH levels below 6.3. The pH of the nanocellulose used in this investigation is 8.7, indicating that it has a negative charge. Consequently, the adsorption of anionic contaminants by this negatively charged nanocellulose is ineffective. Tsade et al. 2021 inquiry, Preparation, and Characterization of Functionalized Cellulose Nanomaterials (CNMs) for Pb(II) Ions Removal from Wastewater, revealed a pH_{PZC} value of 5 for CNMs, corroborating this conclusion.

Thermal stability of SCBNFC

Ensuring thermal stability is essential when utilizing CNF in composite materials. The temperature features Tonset and Td can be calculated from the TGA a reduction in mass curve and the resulting derivative curve with temperature. The degradation characteristics of nanofiber samples derived from sugarcane bagasse cellulose were analyzed thermogravimetrically to compare their behavior at different numbers of passes (K. Zhang et al. 2018). Thermogravimetric (TG) and derivative thermogravimetric (DTG) profiles of the SCBNFC nanofiber samples are illustrated in Figures 7 and 8. Some SCBNFC nanofibers experience a decrease in weight when exposed to temperatures between 20.8°C and 96°C. This weight loss is mostly

Table 5. Dimension size of SCBNFC samples analyzed by TEM microscopies.

Sample	Diameter size mean ± SD (nm)
SCBNFC-5	12.32 ± 2.37 nm
SCBNFC-10	14.07 ± 5.73 nm
SCBNFC-15	13.85 ± 2.86 nm
SCBNFC-20	12.78 ± 2.69 nm

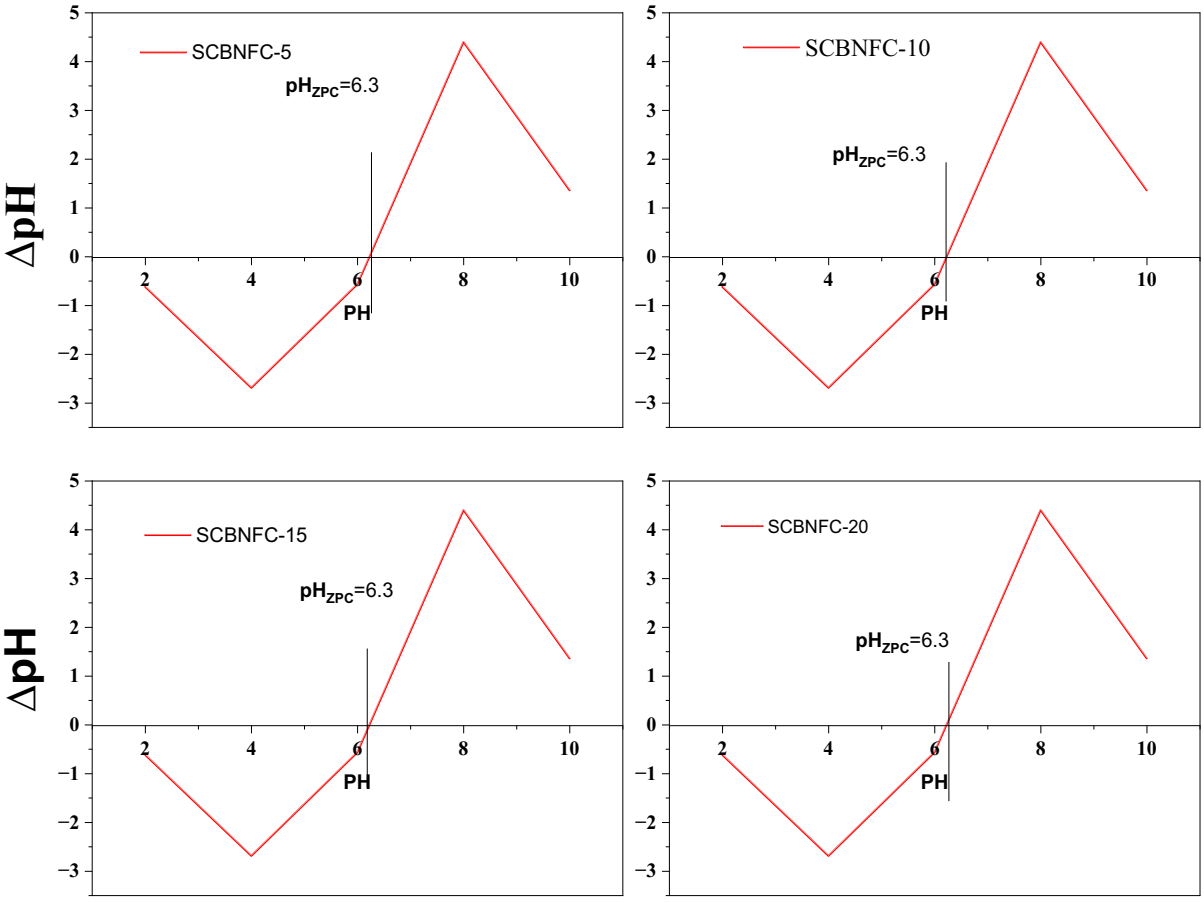

Figure 6. Point of zero charge for SCBNFC samples.

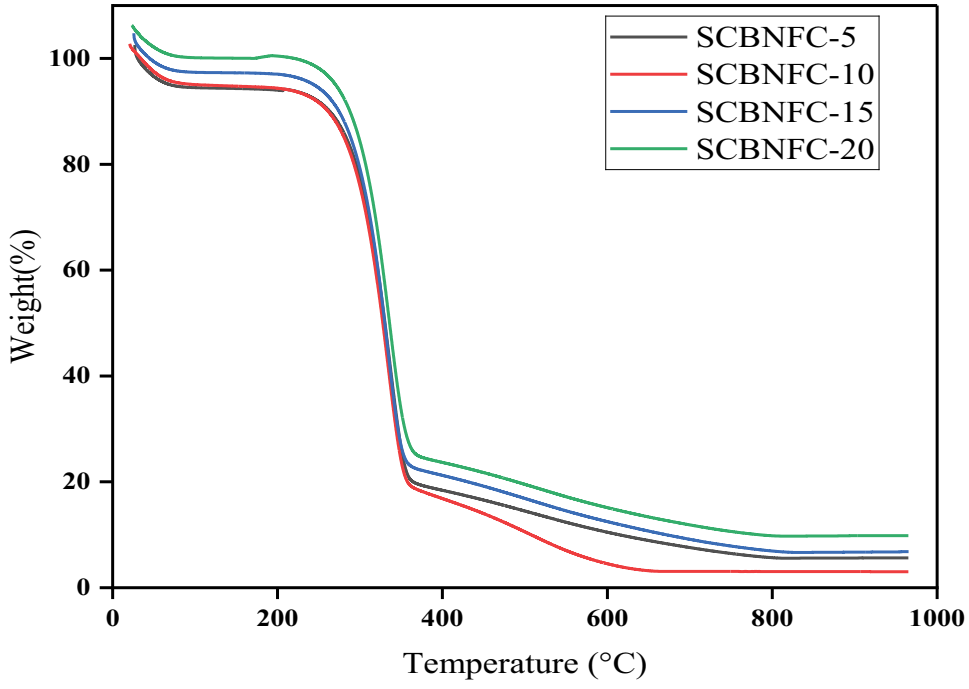

Figure 7. TGA curves for SCBNFC samples.

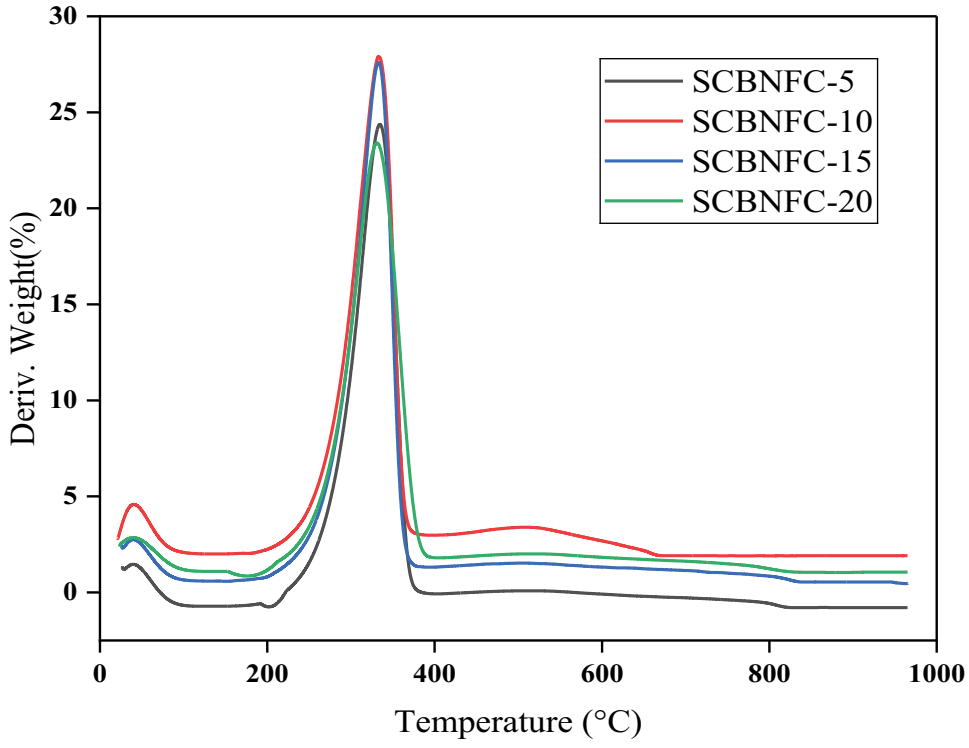

Figure 8. DTG curves for SCBNFC samples.

Table 6. Onset temperature (T_{Onset}), degradation temperature on maximum weight-loss rate (T_{Max}), weight loss (W_L), and char yield for SCBNFC-5, SCBNFC-10, SCBNFC-15, and SCBNFC-20 obtained from the TG and DTG curves.

	Water Evaporation			1st thermal degradation			Char yield
Sample	T_{Onset} (°C)	T_{Max} (°C)	W_L (%)	T_{Onset} (°C)	T_{Max} (°C)	W_L (%)	W (%)
SCBNFC-5	26.9	94.3	8.5	360	826	73.46	17.6
SCBNFC-10	20.8	92.23	7.83	358.6	658.3	75.02	18.1
SCBNFC-15	25.9	92.4	7.73	355.9	817.2	72.15	18.8
SCBNFC-20	23.3	93.18	8.3	364.4	785.3	74.64	17.9

caused by the evaporation of any leftover moisture present in the nanocellulose samples (Ilyas et al. 2019). In addition, the SCBNFC samples showed a consistent thermal degradation range from 355.9°C to 826°C, primarily due to the breakdown of the α-cellulosic chain. The thermogravimetric (TG) analysis data in Table 6 indicate that SCBNFC-10 and SCBNFC-15 exhibited the lowest onset thermal decomposition temperatures, measuring at 92.23°C and 92.4°C, respectively. The variation in crystalline structure organization may be a result of the defibrillation processes, as suggested by Ilyas et al. 2018. For example, the precise arrangement of crystallites in SCBNFC-5 and the altered structure of crystallites in SCBNFC-20 have an impact on its ability to withstand high temperatures before decomposing. In the initial phase of thermal decomposition, SCBNFC-5 and SCBNFC-20 demonstrated higher thermal decomposition temperatures, reaching up to 360°C and 364.4°C, respectively, in comparison to SCBNFC-10 and SCBNFC-15. At a temperature of approximately 370°C, SCBNFC-20 showed the most consistent curve and the highest thermal stability at 195°C and 364.4°C. The enhanced stability of SCBNFC-15 is due to the strong and undisturbed crystal structure, as noted by Ilyas et al. 2018.

Limitation of study

While this study demonstrates the effective isolation and detailed physicochemical characterization of SCBNFC via WDM, several inherent limitations should be critically acknowledged. First, the WDM process was evaluated primarily in terms of fibrillation efficiency and yield, while the associated energy

consumption was not quantified. Given that mechanical nanofibrillation is widely recognized as an energy-intensive process, the absence of specific energy demand analysis limits a rigorous assessment of the process sustainability and industrial scalability. Future investigations incorporating energy – property relationships would be necessary to establish the techno-economic feasibility of WDM-derived SCBNFC.

Second, crystallinity changes were assessed using the Segal method, which provides a relative crystallinity index but does not fully capture structural disorder, crystallite size distribution, or cellulose polymorphic transitions induced by intensive mechanical treatment. The observed reduction in crystallinity with increasing milling cycles should therefore be interpreted with caution, and complementary techniques such as solid-state NMR or advanced X-ray scattering methods would enable a more definitive structural interpretation. Additionally, the study employed sugarcane bagasse obtained from a single geographical source. Variations in agronomic conditions, fiber maturity, and chemical composition are known to influence cellulose structure and fibrillation behavior. Consequently, the reproducibility and broader applicability of the reported findings may be constrained, and future studies involving multi-source feedstocks are warranted.

Conclusion

This study demonstrated the efficiency and sustainability of the WDM method for extracting NFC from SCBF. Although the production of SCBNFC-20 (98.4) decreased slightly, the chemical structure of the nanofibers remained stable after numerous WDM runs. Notably, the WDM treatment had minimal influence on the chemical composition of SCBNFC, even after several cycles, which can be attributed to the complete fibrillation of certain fibers into nanofibers. Each SCBNFC sample also exhibited a negative zeta potential, indicating advantageous stability that effectively prevents nanocellulose from aggregating and encourages the formation of a robust adhesion network of nanofibers within the polymer composite matrix. The TGA study demonstrated that all cycles of SCBNFC possess outstanding thermal stability, indicating that it can withstand high temperatures during composite production. The results of the characterization study suggest that WDM is a promising and viable method for isolating NFC from SCBF. Furthermore, the environmentally conscious development of SCBNFC via WDM highlights its potential for a sustainable and reliable nano-fibrillation approach. The SCBNFC developed in this study is intended for incorporation into thermoplastic elastomer nanocomposites, with a specific focus on its potential application in membrane filtration.

Acknowledgments

The authors would like to extend their sincere appreciation to the Universiti Teknologi Malaysia and the Libyan government for their indispensable support during the duration of this research endeavor. The authors would like to express gratitude for the financial support received from the Universiti Teknologi Malaysia for the project "Modified Areca Catechu Nanocellulose/Nanolignin Reinforced Polylactic Acid Hybrid Nanocomposite Flame Retardant", grant number PY/2025/00526-Q.J130000.5346.01L02. The authors gratefully acknowledge the financial support provided by the ASEAN-INDIA Science & Technology Development Fund (AISTDF) for the project titled "Development of Self-Assembled Nanohybrids of Nickel-Cobalt-Based Layered Double Hydroxides and Graphitic-Carbon Nitrite for Supercapacitor and Water Splitting Application" PY/2025/00780—S.J130000.7646.4Y365. The authors also acknowledge financial support funded by Kurita Water and Environment Foundation (Japan) through the Kurita Overseas Research Grant 2024 (24Pmy108 and PY/2024/01977; 24Pmy107 and PY/2024/01976). The author would like to acknowledge Putra Inisiatif Grant (9755300), Universiti Putra Malaysia and Universiti Pertahanan Nasional for the financial support.

Author contributions

CRediT: **Asmaa Ali Mubarak:** Conceptualization, Data curation, Formal analysis, Methodology, Validation, Writing – original draft; **R.A. Ilyas:** Conceptualization, Data curation, Formal analysis, Funding acquisition, Methodology, Writing – original draft; **Faris M. AL-Oqla:** Conceptualization, Methodology, Writing – original draft, Writing – review & editing; **Norzita Ngadi:** Data curation, Formal analysis, Writing – original draft; **Abu Hassan Nordin:** Conceptualization, Formal analysis, Writing – original draft; **M.F.M. Alkbir:** Conceptualization, Investigation, Validation, Writing – original draft; **Nadlene Razali:** Data curation, Formal analysis, Investigation, Writing – original draft; **S.M. Sapuan:** Conceptualization, Formal analysis, Investigation, Methodology, Supervision, Writing – original

draft; **Mohd nor Faiz Norrrahim:** Conceptualization, Formal analysis, Investigation, Writing – original draft; **Victor Feizal Knight:** Conceptualization, Formal analysis, Funding acquisition, Validation, Writing – original draft.

Author contribution declaration

Author A.A.M. drafted the original manuscript. Authors A.A.M., R.A.I., F.M.A., N.N., and A.H.N. revised the manuscript, while author A.A.M conceptualized the idea of the manuscript.

Disclosure statement

No potential conflict of interest was reported by the author(s).

Funding

We thank Universiti Teknologi Malaysia for funding the research "The influence of chemical and fibre traits of Malaysian bamboos on their pulp and paper characteristics" under grant number [PY/2022/02318—Q. J130000.3851.21H99]. The research has been carried out under the program, Research Excellence Consortium (JPT (BPKI) 1000/016/018/25 (57)), provided by the Ministry of Higher Education (MOHE) Malaysia.

Availability of data and Materials

This study article includes all essential data and resources.

References

Abdel-Hakim, A., and R. Mourad. 2023. "Nanocellulose and Its Polymer Composites: Preparation, Characterization, and Applications." *Russian Chemical Reviews* 92 (4): RCR5076. https://doi.org/10.57634/rcr5076.

Abdullah, N. A., M. S. A. Rani, M. Mohammad, M. H. Sainorudin, N. Asim, Z. Yaakob, H. Razali, and Z. Emdadi. 2021. "Nanocellulose from Agricultural Waste as an Emerging Nanotechnology Material for Nanotechnology Applications - An Overview." *Polimery/Polymers* 66 (3): 157–168. https://doi.org/10.14314/POLIMERY.2021.3.1.

Abral, H., M. K. Chairani, M. D. Rizki, M. Mahardika, D. Handayani, E. Sugiarti, A. N. Muslimin, S. M. Sapuan, and R. A. Ilyas. 2021. "Characterization of Compressed Bacterial Cellulose Nanopaper Film After Exposure to Dry and Humid Conditions." *Journal of Materials Research and Technology* 11:896–904. https://doi.org/10.1016/j.jmrt.2021.01.057.

Anitha, R., R. Brindavathy, N. Sritharan, N. Jagathjothi, R. S. Priya, M. Yuvaraj, C. Jaiby, et al. 2024. "Comparative Efficacy of Sodium Metasilicate and Organic Source Combination on Sugarcane (Saccharum officinarum L.) for Reducing the Post-Harvest Deterioration Losses." *Silicon* 16 (1): 425–434. https://doi.org/10.1007/s12633-023-02679-x.

Arisyah, T., T. Yasim-Anuar, H. Ariffin, M. Nor, F. Norrrahim, and M. A. Hassan. 2017. "Factors Affecting Spinnability of Oil Palm Mesocarp Fiber Cellulose Solution for the Production of Microfiber." *BioResources* 12 (1): 715–734. https://doi.org/10.15376/biores.12.1.715-734.

Asmaa Ali Mubarak, R. A. I., A. H. Ngadi, N. Nordin, M. F. M. Alkbir, and M. F. M. Alkbir. 2024. "Isolation and Characterization of Cellulose from Sugarcane Bagasse Fiber (Saccharum officinarum) via Delignification and Mercerization Treatment Using Response Surface Modeling (RSM)." *Biomass Conversion and Biorefinery* 15 (19): 26485–26499. https://doi.org/10.1007/s13399-024-05692-1.

Dai, L., Y. Wang, X. Zou, Z. Chen, H. Liu, and Y. Ni. 2020. "Ultrasensitive Physical, Bio, and Chemical Sensors Derived from 1-, 2-, and 3-D Nanocellulosic Materials." *Small* 16 (13). https://doi.org/10.1002/smll.201906567.

Del Cerro, D. R., T. V. Koso, T. Kakko, A. W. T. King, and I. Kilpeläinen. 2020. "Crystallinity Reduction and Enhancement in the Chemical Reactivity of Cellulose by Non-Dissolving Pre-Treatment with Tetrabutylphosphonium Acetate." *Cellulose* 27 (10): 5545–5562. https://doi.org/10.1007/s10570-020-03044-6.

de Santana, J. E., F. G. S. de Andrade, A. F. Ferreira, M. G. Ghislandi, and M. A. da. 2024. "Motta Sobrinho, Isotherms, Kinetics and Thermodynamics of Industrial Dye Acid Red 27 Adsorption on Sugarcane Bagasse Ash." *Environmental Science and Pollution Research* 31 (41): 53691–53705. https://doi.org/10.1007/s11356-024-31917-x.

Devarajan, M. M., G. Kumaraguruparan, K. J. Nagarajan, and C. Vignesh. 2024. "Production of Hybrid AgNPs - TEMPO-Mediated Oxidation Cellulose Composite from Jackfruit Peduncle Agro-Waste and Its Thermal Management Application in Electronic Devices." *International Journal of Biological Macromolecules* 254:127848. https://doi.org/10.1016/j.ijbiomac.2023.127848.

Diharjo, K., F. Gapsari, A. Andoko, R. Septiari, S. M. Rangappa, and S. Siengchin. 2023. "Optimization of Nano Cellulose Extraction from Timoho Fiber Using Response Surface Methodology (RSM)." *Biomass Conversion and Biorefinery* 14 (20): 25557–25567. https://doi.org/10.1007/s13399-023-04551-9.

Dominic, C. D., R. Joseph, P. M. S. Begum, M. Joseph, D. Padmanabhan, L. A. Morris, A. S. Kumar, and K. Formela. 2020. "Cellulose Nanofibers Isolated from the Cuscuta reflexa Plant as a Green Reinforcement of Natural Rubber." *Polymers (Basel)* 12 (4): 814. https://doi.org/10.3390/polym12040814.

Dufresne, A., D. Danie`, D. Dupeyre, and M. R. Vignon. 2000. "Cellulose Microfibrils from Potato Tuber Cells: Processing and Characterization of Starch-Cellulose Microfibril Composites." *Journal of Applied Polymer Science* 76 (14): 2080–2092. https://doi.org/10.1002/(SICI)1097-4628(20000628)76:14<2080::AID-APP12>3.0.CO;2-U.

Elsayed, I., G. T. Schueneman, E. M. El-Giar, and E. B. Hassan. 2023. "Amino-Functionalized Cellulose Nanofiber/Lignosulfonate New Aerogel Adsorbent for the Removal of Dyes and Heavy Metals from Wastewater." *Gels* 9 (2): 154. https://doi.org/10.3390/gels9020154.

Fahma, F., S. Iwamoto, N. Hori, T. Iwata, and A. Takemura. 2010. "Isolation, Preparation, and Characterization of Nanofibers from Oil Palm Empty-Fruit-Bunch (OPEFB)." *Cellulose* 17 (5): 977–985. https://doi.org/10.1007/s10570-010-9436-4.

Fernandes, A., L. Cruz-Lopes, B. Esteves, and D. Evtuguin. 2023. "Nanotechnology Applied to Cellulosic Materials." *Materials* 16 (8): 3104. https://doi.org/10.3390/ma16083104.

Gan, P. G., S. T. Sam, M. F. B. Abdullah, and M. F. Omar. 2020. "Thermal Properties of Nanocellulose-Reinforced Composites: A Review." *Journal of Applied Polymer Science* 137 (11). https://doi.org/10.1002/app.48544.

Gond, R. K., M. K. Gupta, and M. Jawaid. 2021. "Extraction of Nanocellulose from Sugarcane Bagasse and Its Characterization for Potential Applications." *Polymer Composites* 42 (10): 5400–5412. https://doi.org/10.1002/pc.26232.

Guélon, T., J.-D. Mathias, and P. Stoodley. 2011. *Advances in Biofilm Mechanics*, 111–139. https://doi.org/10.1007/978-3-642-19940-0_6.

Guimarães, I. C., K. C. dos Reis, E. G. T. Menezes, A. C. Rodrigues, T. F. da Silva, I. R. N. de Oliveira, and E. V. de B Vilas Boas. 2016. "Cellulose Microfibrillated Suspension of Carrots Obtained by Mechanical Defibrillation and Their Application in Edible Starch Films, Ind." *Industrial Crops and Products* 89:285–294. https://doi.org/10.1016/j.indcrop.2016.05.024.

Haafiz, M. K. M., A. Hassan, Z. Zakaria, and I. M. Inuwa. 2014. "Isolation and Characterization of Cellulose Nanowhiskers from Oil Palm Biomass Microcrystalline Cellulose, Carbohydr." *Carbohydrate Polymers* 103:119–125. https://doi.org/10.1016/j.carbpol.2013.11.055.

Hassan, M. L., A. P. Mathew, E. A. Hassan, N. A. El-Wakil, and K. Oksman. 2012. "Nanofibers from Bagasse and Rice Straw: Process Optimization and Properties." *Wood Science and Technology* 46 (1–3): 193–205. https://doi.org/10.1007/s00226-010-0373-z.

He, C., H. Li, J. Hong, H. Xiong, H. Ni, and M. Zheng. 2022. "Characterization and Functionality of Cellulose from Pomelo Fruitlets by Different Extraction Methods." *Polymers (Basel)* 14 (3): 518. https://doi.org/10.3390/polym14030518.

Hu, M., X. Lv, Y. Wang, Y. Zhang, and H. Dai. 2024. "Guideline for the Extraction of Nanocellulose from Lignocellulosic Feedstocks." *Food Biomacromolecules* 1 (1): 9–17. https://doi.org/10.1002/fob2.12011.

Ilyas, R. A., S. M. Sapuan, M. S. N. Atikah, M. R. M. Asyraf, S. A. Rafiqah, H. A. Aisyah, N. M. Nurazzi, and M. N. F. Norrrahim. 2021. "Effect of Hydrolysis Time on the Morphological, Physical, Chemical, and Thermal Behavior of Sugar Palm Nanocrystalline Cellulose (Arenga pinnata (Wurmb.) Merr)." *Textile Research Journal* 91 (1–2): 152–167. https://doi.org/10.1177/0040517520932393.

Ilyas, R. A., S. M. Sapuan, and M. R. Ishak. 2018. "Isolation and Characterization of Nanocrystalline Cellulose from Sugar Palm Fibres (Arenga pinnata)." *Carbohydrate Polymers* 181:1038–1051. https://doi.org/10.1016/j.carbpol.2017.11.045.

Ilyas, R. A., S. M. Sapuan, M. R. Ishak, and E. S. Zainudin. 2017. "Effect of Delignification on the Physical, Thermal, Chemical, and Structural Properties of Sugar Palm Fibre." *Bioresources* 12 (4): 8734–8754. https://doi.org/10.15376/biores.12.4.8734-8754.

Ilyas, R. A., S. M. Sapuan, M. R. Ishak, and E. S. Zainudin. 2019. "Sugar Palm Nanofibrillated Cellulose (Arenga Pinnata (Wurmb.) Merr): Effect of Cycles on Their Yield, Physic-Chemical, Morphological and Thermal Behavior." *International Journal of Biological Macromolecules* 123:379–388. https://doi.org/10.1016/j.ijbiomac.2018.11.124.

Ilyas, R. A., S. M. Sapuan, M. L. Sanyang, M. R. Ishak, and E. S. Zainudin. 2018. "Nanocrystalline Cellulose as Reinforcement for Polymeric Matrix Nanocomposites and Its Potential Applications: A Review." *Current Analytical Chemistry* 14 (3): 203–225. https://doi.org/10.2174/1573411013666171003155624.

Ilyas Rushdana, A., M. Sapuan Salit, M. Lamin Sanyang, and M. Ridzwan Ishak. 2017. "Nanocrystalline Cellulose as Reinforcement for Polymeric Matrix Nanocomposites and Its Potential Applications." *A Review, Current Analytical Chemistry* 14:13. https://doi.org/10.2174/1573411013666171003155624.

Imraan, M., R. A. Ilyas, A. S. Norfarhana, S. P. Bangar, V. F. Knight, and M. N. F. Norrrahim. 2023. "Sugar Palm (Arenga Pinnata) Fibers: New Emerging Natural Fibre and Its Relevant Properties, Treatments and Potential Applications." *Journal of Materials Research and Technology* 24:4551–4572. https://doi.org/10.1016/j.jmrt.2023.04.056.

Ismail, S. O., E. Akpan, and H. N. Dhakal. 2022. "Review on Natural Plant Fibres and Their Hybrid Composites for Structural Applications: Recent Trends and Future Perspectives, Composites Part C: Open Access." *Composites Part C: Open Access* 9:100322. https://doi.org/10.1016/j.jcomc.2022.100322.

Jonasson, S., A. Bünder, T. Niittylä, and K. Oksman. 2020. "Isolation and Characterization of Cellulose Nanofibers from Aspen Wood Using Derivatizing and Non-Derivatizing Pretreatments." *Cellulose* 27 (1): 185–203. https://doi.org/10.1007/s10570-019-02754-w.

Khan, M. N., N. Rehman, A. Sharif, E. Ahmed, Z. H. Farooqi, and M. I. Din. 2020. "Environmentally Benign Extraction of Cellulose from Dunchi Fiber for Nanocellulose Fabrication." *International Journal of Biological Macromolecules* 153:72–78. https://doi.org/10.1016/j.ijbiomac.2020.02.333.

Kumar Trivedi, A., A. Kumar, and M. K. Gupta. 2023. "Extraction of Nanocellulose from Wheat Straw and Its Characterization." *Materials Today: Proceedings* 78:48–54. https://doi.org/10.1016/j.matpr.2022.11.038.

Li, B., W. Xu, D. Kronlund, J.-E. Eriksson, A. Määttänen, S. Willför, and C. Xu. 2018. "Comparable Characterization of Nanocellulose Extracted from Bleached Softwood and Hardwood Pulps." *Paper and Biomaterials* 3 (4): 35–44. https://doi.org/10.26599/pbm.2018.9260026.

Llanos, J. H. R., and C. C. Tadini. 2018. "Preparation and Characterization of Bio-Nanocomposite Films Based on Cassava Starch or Chitosan, Reinforced with Montmorillonite or Bamboo Nanofibers." *International Journal of Biological Macromolecules* 107:371–382. https://doi.org/10.1016/j.ijbiomac.2017.09.001.

Lu, Y., P. Tao, N. Zhang, and S. Nie. 2020. "Preparation and Thermal Stability Evaluation of Cellulose Nanofibrils from Bagasse Pulp with Differing Hemicelluloses Contents." *Carbohydrate Polymers* 245:116463. https://doi.org/10.1016/j.carbpol.2020.116463.

Mahur, B. K., A. Ahuja, S. Singh, P. K. Maji, and V. K. Rastogi. 2023. "Different Nanocellulose Morphologies (Cellulose Nanofibers, Nanocrystals and Nanospheres) Extracted from Sunn Hemp (Crotalaria juncea)." *International Journal of Biological Macromolecules* 253:126657. https://doi.org/10.1016/j.ijbiomac.2023.126657.

Mandal, A., and D. Chakrabarty. 2011. "Isolation of Nanocellulose from Waste Sugarcane Bagasse (SCB) and Its Characterization" *Carbohydrate Polymers* 86 (3): 1291–1299. https://doi.org/10.1016/j.carbpol.2011.06.030.

Masruchin, N., P. Amanda, W. B. Kusumaningrum, L. Suryanegara, and A. Nuryawan. 2020. "Particle Size Distribution and Yield Analysis of Different Charged Cellulose Nanofibrils Obtained by TEMPO-Mediated Oxidation." *IOP Conference Series: Earth and Environmental Science* 572: 012045. https://doi.org/10.1088/1755-1315/572/1/012045.

Mayerberger, E. A., R. M. Street, R. M. McDaniel, M. W. Barsoum, and C. L. Schauer. 2018. "Antibacterial Properties of Electrospun Ti $_3C_2$Tz (MXene)/Chitosan Nanofibers." *RSC Advances* https://doi.org/10.1039/C8RA06274A.

Mehanny, S., E. E. Abu-El Magd, M. Ibrahim, M. Farag, R. Gil-San-Millan, J. Navarro, A. E. H. El Habbak, and E. El-Kashif. 2021. "Extraction and Characterization of Nanocellulose from Three Types of Palm Residues." *Journal of Materials Research and Technology* 10:526–537. https://doi.org/10.1016/j.jmrt.2020.12.027.

Midhun Dominic, C. D., V. Raj, K. V. Neenu, P. M. S. Begum, K. Formela, M. R. Saeb, D. D. Prabhu, P. Poornima Vijayan, T. G. Ajithkumar, and J. Parameswaranpillai. 2022. "Chlorine-Free Extraction and Structural Characterization of Cellulose Nanofibers from Waste Husk of Millet (Pennisetum glaucum)." *International Journal of Biological Macromolecules* 206:92–104. https://doi.org/10.1016/j.ijbiomac.2022.02.078.

Nazrin, A., S. M. Sapuan, M. Y. M. Zuhri, I. S. M. A. Tawakkal, and R. A. Ilyas. 2021. "Water Barrier and Mechanical Properties of Sugar Palm Crystalline Nanocellulose Reinforced Thermoplastic Sugar Palm Starch (TPS)/Poly(Lactic Acid) (PLA) Blend Bionanocomposites." *Nanotechnology Review* 10 (1): 431–442. https://doi.org/10.1515/ntrev-2021-0033.

Nguyen, C. T. X., K. H. Bui, B. Y. Truong, N. H. N. Do, and P. T. K. Le. 2021. "Nanocellulose from Pineapple Leaf and Its Applications Towards High-Value Engineering Materials." *Chemical Engineering Transactions* 89:19–24. https://doi.org/10.3303/CET2189004.

Ning, F., X. Li, N. O. Hear, R. Zhou, C. Shi, and X. Ning. 2019. "Thermal Failure Mechanism of Fiber Ropes When Bent Over Sheaves." *Textile Research Journal* 89 (7): 1215–1223. https://doi.org/10.1177/0040517518767147.

Norfarhana, A. S., R. A. Ilyas, N. Ngadi, and M. H. Dzarfan Othman. 2024. "Innovative Ionic Liquid Pretreatment Followed by Wet Disk Milling Treatment Provides Enhanced Properties of Sugar Palm Nano-Fibrillated Cellulose." *Heliyon* 10 (6): e27715. https://doi.org/10.1016/j.heliyon.2024.e27715.

Norrrahim, M. N. F., H. Ariffin, M. A. Hassan, N. A. Ibrahim, W. M. Z. W. Yunus, and H. Nishida. 2019. "Utilisation of Superheated Steam in Oil Palm Biomass Pretreatment Process for Reduced Chemical Use and Enhanced Cellulose Nanofibre Production." *International Journal of Nanotechnology* 16 (11/12): 668. https://doi.org/10.1504/IJNT.2019.107360.

Norrrahim, M. N. F., H. Ariffin, T. A. T. Yasim-Anuar, F. Ghaemi, M. A. Hassan, N. A. Ibrahim, J. L. H. Ngee, and W. M. Z. W. Yunus. 2018. "Superheated Steam Pretreatment of Cellulose Affects Its Electrospinnability for Microfibrillated Cellulose Production." *Cellulose* 25 (7): 3853–3859. https://doi.org/10.1007/s10570-018-1859-3.

Oun, A. A., and J. W. Rhim. 2018. "Isolation of Oxidized Nanocellulose from Rice Straw Using the Ammonium Persulfate Method." *Cellulose* 25 (4): 2143–2149. https://doi.org/10.1007/s10570-018-1730-6.

Pelissari, F. M., M. M. Andrade-Mahecha, P. J. Do A Sobral, and F. C. Menegalli. 2017a. "Nanocomposites Based on Banana Starch Reinforced with Cellulose Nanofibers Isolated from Banana Peels." *Journal of Colloid and Interface Science* 505:154–167. https://doi.org/10.1016/j.jcis.2017.05.106.

Pelissari, F. M., M. M. Andrade-Mahecha, P. J. Do A Sobral, and F. C. Menegalli. 2017b. "Nanocomposites Based on Banana Starch Reinforced with Cellulose Nanofibers Isolated from Banana Peels." *Journal of Colloid Interface Science* 505:154–167. https://doi.org/10.1016/j.jcis.2017.05.106.

Phanthong, P., P. Reubroycharoen, X. Hao, G. Xu, A. Abudula, and G. Guan. 2018. "Nanocellulose: Extraction and Application, Carbon Resources Conversion." *Carbon Resources Conversion* 1 (1): 32–43. https://doi.org/10.1016/j.crcon.2018.05.004.

Potthast, A., K. Ahn, M. Becker, T. Eichinger, M. Kostic, S. Böhmdorfer, M. J. Jeong, and T. Rosenau. 2022. "Acetylation of Cellulose – Another Pathway of Natural Cellulose Aging During Library Storage of Books and Papers, Carbohydr." *Carbohydrate Polymers* 287:119323. https://doi.org/10.1016/j.carbpol.2022.119323.

Rajan, S. T. K., K. J. Nagarajan, V. Balasubramani, K. Sathickbasha, M. R. Sanjay, S. Siengchin, and A. N. Balaji. 2023. "Investigation of Mechanical and Thermo-Mechanical Characteristics of Silane-Treated Cellulose Nanofibers from Agricultural Waste Reinforced Epoxy Adhesive Composites." *International Journal of Adhesion and Adhesives* 126:103492. https://doi.org/10.1016/j.ijadhadh.2023.103492.

Ramki, S., R. Sukanya, S.-M. Chen, and M. Sakthivel. 2019. "Hierarchical Multi-Layered Molybdenum Carbide Encapsulated Oxidized Carbon Nanofiber for Selective Electrochemical Detection of Antimicrobial Agents: Inter-Connected Path in Multi-Layered Structure for Efficient Electron Transfer." *Inorganic Chemistry Frontiers* 6 (7): 1680–1693. https://doi.org/10.1039/C9QI00158A.

Rana, M. M., and H. De la Hoz Siegler. 2023. "H. De La Hoz Siegler, Influence of Ionic Liquid (IL) Treatment Conditions in the Regeneration of Cellulose with Different Crystallinity." *Journal of Materials Research* 38 (2): 328–336. https://doi.org/10.1557/s43578-022-00797-7.

Reshmy, R., E. Philip, S. A. Paul, A. Madhavan, R. Sindhu, P. Binod, A. Pandey, and R. Sirohi. 2020. "Nanocellulose-Based Products for Sustainable Applications-Recent Trends and Possibilities." *Reviews in Environmental Science and Bio/Technology* 19 (4): 779–806. https://doi.org/10.1007/s11157-020-09551-z.

Samsalee, N., J. Meerasri, and R. Sothornvit. 2023. "Rice Husk Nanocellulose: Extraction by High-Pressure Homogenization, Chemical Treatments and Characterization." *Carbohydrate Polymer Technologies and Applications* 6:100353. https://doi.org/10.1016/j.carpta.2023.100353.

Sapuan, S. M., M. Lamin Sanyang, and M. Ridzwan Ishak. 2016. "Nanocrystalline Cellulose Reinforced Starch-Based Nanocomposites." *A Review*. https://www.researchgate.net/publication/315675302 .

Segal, L., J. J. Creely, A. E. Martin, and C. M. Conrad. 1952. "Opportunity for New Developments in All Phases of Textile Manufacturing. ' Literature Cited an Empirical Method for Estimating the Degree of Crystallinity of Native Cellulose Using the X-Ray Diffractometer." *Textile Research Journal* 29 (10): 786–794. https://doi.org/10.1177/004051755902901O.

Sheltami, R. M., I. Abdullah, I. Ahmad, A. Dufresne, and H. Kargarzadeh. 2012. "Extraction of Cellulose Nanocrystals from Mengkuang Leaves (Pandanus tectorius)." *Carbohydrate Polymers* 88 (2): 772–779. https://doi.org/10.1016/j.carbpol.2012.01.062.

Shirani, S., J. Varshosaz, M. Rostami, and M. Mirian. 2022. "Redox Responsive Polymeric Micelles of Gellan Gum/Abietic Acid for Targeted Delivery of Ribociclib." *International Journal of Biological Macromolecules* 215:334–345. https://doi.org/10.1016/j.ijbiomac.2022.06.095.

Sihag, S., M. Y. Sheetal, and J. Pal. 2022. "Extraction and Characterization of Nanocellulose from Wheat Straw: Facile Approach." *Journal of Water and Environmental Nanotechnology* 7:317–331. https://doi.org/10.22090/jwent.2022.03.007.

Souza, A. G., D. F. Santos, R. R. Ferreira, V. Z. Pinto, and D. S. Rosa. 2020. "Innovative Process for Obtaining Modified Nanocellulose from Soybean Straw." *International Journal of Biological Macromolecules* 165:1803–1812. https://doi.org/10.1016/j.ijbiomac.2020.10.036.

Sun, Y. Y., Z. P. Xia, A. P. Yang, J. X. Li, L. Wang, H. Chen, X. Zheng, and Y. Liu. 2021. "Nanocellulose Extracted from Waste Polyester/Cotton Fabric by Chemical-Mechanical Separation Technology." *Journal of Physics: Conference Series* 1:012074. https://doi.org/10.1088/1742-6596/1790/1/012074.

Supian, M. A. F., K. N. M. Amin, S. S. Jamari, and S. Mohamad. 2020. "Production of Cellulose Nanofiber (CNF) from Empty Fruit Bunch (EFB) via Mechanical Method." *Journal of Environmental Chemical Engineering* 8 (1): 103024. https://doi.org/10.1016/j.jece.2019.103024.

Syafri, E., N. H. S. Jamaluddin, P. Mahardika, M. Amanda, R. A. Ilyas. 2022a. "Isolation and Characterization of Cellulose Nanofibers from Agave gigantea by Chemical-Mechanical Treatment." *International Journal of Biological Macromolecules* 200:25–33. https://doi.org/10.1016/j.ijbiomac.2021.12.111.

Syafri, E., N. H. S. Jamaluddin, P. Mahardika, M. Amanda, and R. A. Ilyas. 2022b. "Isolation and Characterization of Cellulose Nanofibers from Agave gigantea by Chemical-Mechanical Treatment." *International Journal of Biological Macromolecules* 200:25–33. https://doi.org/10.1016/j.ijbiomac.2021.12.111.

Taflick, T., L. A. Schwendler, S. M. L. Rosa, C. I. D. Bica, and S. M. B. Nachtigall. 2017. "Cellulose Nanocrystals from Acacia Bark–Influence of Solvent Extraction." *International Journal of Biological Macromolecules* 101:553–561. https://doi.org/10.1016/j.ijbiomac.2017.03.076.

Tonoli, G. H. D., A. P. Joaquim, M. A. Arsne, K. Bilba, and H. Savastano. 2007. "Performance and Durability of Cement Based Composites Reinforced with Refined Sisal Pulp." *Materials & Manufacturing Processes* 22 (2): 149–156. https://doi.org/10.1080/10426910601062065.

Tsade, H., S. T. Anshebo, and F. K. Sabir. 2021. "Preparation and Characterization of Functionalized Cellulose Nanomaterials (CNMs) for Pb(II) Ions Removal from Wastewater." *Journal of Chemistry* 2021:1–18. https://doi.org/10.1155/2021/5514853.

Valdebenito, F., M. Pereira, G. Ciudad, L. Azocar, R. Briones, and G. Chinga-Carrasco. 2017. "On the Nanofibrillation of Corn Husks and Oat Hulls Fibres, Ind." *Crops Prod* 95:528–534. https://doi.org/10.1016/j.indcrop.2016.11.006.

Wang, Q. Q., J. Y. Zhu, R. Gleisner, T. A. Kuster, U. Baxa, and S. E. McNeil. 2012. "Morphological Development of Cellulose Fibrils of a Bleached Eucalyptus Pulp by Mechanical Fibrillation." *Cellulose* 19 (5): 1631–1643. https://doi.org/10.1007/s10570-012-9745-x.

Wang, Y., Y. Yu, S. Hu, J. Yu, Y. Huang, and H. Dai. 2025. "Preparation of Agrowaste-Based Nanocellulose by NaOH-Assisted Ball Milling Technique: Influence of Component Intervention." *Gels* 11 (8): 631. https://doi.org/10.3390/gels11080631.

Xie, J., C. Y. Hse, C. F. De Hoop, T. Hu, J. Qi, and T. F. Shupe. 2016. "Isolation and Characterization of Cellulose Nanofibers from Bamboo Using Microwave Liquefaction Combined with Chemical Treatment and Ultrasonication, Carbohydr." *Carbohydrate Polymers* 151:725–734. https://doi.org/10.1016/j.carbpol.2016.06.011.

Xing, J., P. Tao, Z. Wu, C. Xing, X. Liao, and S. Nie. 2019. "Nanocellulose-Graphene Composites: A Promising Nanomaterial for Flexible Supercapacitors, Carbohydr." *Carbohydrate Polymers* 207:447–459. https://doi.org/10.1016/j.carbpol.2018.12.010.

Yasim-Anuar, T. A. T., N. S. Sharip, L. N. Megashah, H. Ariffin, and N. A. M. Nor. 2020a. "Cellulose Nanofibers from Waste Paper and Their Utilization as Reinforcement Materials in Poly((R)-3-Hydroxybutyrate-Co-(R)-3-Hydroxyhexanoate Bionanocomposite." *Pertanika Journal of Science and Technology* 28 (S2): 259–271. https://doi.org/10.47836/pjst.28.S2.20.

Yasim-Anuar, T. A. T., N. S. Sharip, L. N. Megashah, H. Ariffin, and N. A. M. Nor. 2020b. "Cellulose Nanofibers from Waste Paper and Their Utilization as Reinforcement Materials in Poly((R)-3-Hydroxybutyrate-Co-(R)-3-Hydroxyhexanoate Bionanocomposite." *Pertanika Journal of Science Technology* 28 (S2): 259–271. https://doi.org/10.47836/pjst.28.S2.20.

Yasim-Anuar, T. A. T., N. S. Sharip, L. N. Megashah, H. Ariffin, and N. A. M. Nor. 2020c. "Reinforcement Materials in Poly((R)-3-Hydroxybutyrate-Co-(R)-3-Hydroxyhexanoate Bionanocomposite." *Pertanika Journal of Science and Technology* 28 (S2). https://doi.org/10.47836/pjst.28.s2.20.

Zhang, H., S. Nie, C. Qin, and S. Wang. 2019. "Removal of Hexenuronic Acid to Reduce AOX Formation in Hot Chlorine Dioxide Bleaching of Bagasse Pulp, Ind." *Industrial Crops and Products* 128:338–345. https://doi.org/10.1016/j.indcrop.2018.11.025.

Zhang, K., Y. Zhang, D. Yan, C. Zhang, and S. Nie. 2018. "Enzyme-Assisted Mechanical Production of Cellulose Nanofibrils: Thermal Stability." *Cellulose* 25 (9): 5049–5061. https://doi.org/10.1007/s10570-018-1928-7.

Zhang, S., X. Feng, Y. Huang, Y. Wang, H. Chen, Y. Yu, L. Ma, Y. Zhang, and H. Dai. 2022. "Facile Isolation of Cellulose Nanofibrils from Agro-Processing Residues and Its Improved Stabilization Effect on Gelatin Emulsion." *International Journal of Biological Macromolecules* 216:272–281. https://doi.org/10.1016/j.ijbiomac.2022.07.005.